Collection SFN **7** (2007) s123–s143

The uses of polarisation analysis in the determination of magnetic structure

P.J. Brown[1]

[1] *Institut Laue Langevin, BP. 156X, 38042 Grenoble Cedex, France*
and
Physics Department, Loughborough University, Loughborough, UK

Abstract. This lecture addresses the application of polarimetry, and in paricular *spherical neutron polarimetry* (SNP) to the determination of magnetic structures. The first section introduces some of the fundamental equations, and shows how they relate to the quantities measured using polarisation analysis. Then the problems which may be encountered when dealing with real crystals are introduced. The final sections provide some examples of problems to which SNP has been succesfully applied.

1 NOTATIONS

$\mathbf{P}$	Input polarisation vector
P_i	i^{th} component of input polarisation
$\mathbf{P}'$	Scattered polarisation vector
P'_i	i^{th} component of scattered polarisation
$\mathbf{P}''$	Polarisation created by scattering
P''_i	i^{th} component of polarisation created by scattering
P	Polarisation matrix
$\mathcal{P}$	Polarisation tensor
$\mathcal{P}_{ij}$	ij^{th} element of the polarisation tensor
$F_N(\mathbf{Q})$	Nuclear structure factor for reflection at $\mathbf{Q}$
F_N	Abbreviation for $F_N(\mathbf{Q})$
F_N^*	Complex conjugate of F_N
$F_N^*(\mathbf{Q})$	Complex conjugate of $F_N(\mathbf{Q})$
$\mathbf{F}_{\mathbf{M}}(\mathbf{Q})$	Magnetic structure factor for reflection at $\mathbf{Q}$
$\mathbf{M}_\perp(\mathbf{Q})$	Magnetic interaction vector for reflection at $\mathbf{Q}$
$\mathbf{M}_\perp^*(\mathbf{Q})$	Complex conjugate of $\mathbf{M}_\perp(\mathbf{Q})$
$\mathbf{M}_\perp$	Abbreviation for $\mathbf{M}_\perp(\mathbf{Q})$
$\mathbf{M}_\perp^*$	Complex conjugate of $\mathbf{M}_\perp$
$M_{\perp i}$	i^{th} component of magnetic interaction vector
$M_\perp$	Modulus of magnetic interaction vector
$\boldsymbol{\tau}$	Magnetic propagation vector
$\mathbf{M}(\mathbf{r})$	Magnetisation distribution
$\mathbf{g}$	Reciprocal lattice vector
$\boldsymbol{l}$	Crystal lattice vector
$\mathbf{r}$	Radius vector in real space

Q	Scattering vector = $k_i - k_f$
$\boldsymbol{\kappa}$	Crystallographic scattering vector =$-\mathbf{Q}$

2 VECTOR PROPERTIES OF NEUTRON SCATTERING

2.1 The magnetic interaction vector

Consider just a dipole-dipole interaction between the neutron's spin and a vector field $\mathbf{A}(\mathbf{r})$. If the incident polarisation vector is $\mathbf{P}$, $\mathbf{P}'$ is the polarisation scattered with scattering vector $\mathbf{Q}$ and I is proportional to the scattered intensity then

$$\begin{aligned}\mathbf{P}'I = {} & \mathbf{A}(\mathbf{Q})(\mathbf{P}\cdot\mathbf{A}^*(\mathbf{Q})) + \mathbf{A}^*(\mathbf{Q})(\mathbf{P}\cdot\mathbf{A}(\mathbf{Q})) \\ & -\mathbf{P}(\mathbf{A}(\mathbf{Q})\cdot\mathbf{A}^*(\mathbf{Q})) + i(\mathbf{A}(\mathbf{Q})\times\mathbf{A}^*(\mathbf{Q}))\end{aligned} \tag{2.1}$$

and

$$I = \mathbf{A}(\mathbf{Q})\cdot\mathbf{A}^*(\mathbf{Q}) - i\mathbf{P}\cdot\mathbf{A}(\mathbf{Q})\times\mathbf{A}^*(\mathbf{Q}) \tag{2.2}$$

where $\mathbf{A}(\mathbf{Q})$ is the Q^{th} Fourier component of the vector field $\mathbf{A}(\mathbf{r})$

$$\mathbf{A}(\mathbf{Q}) = \int \mathbf{A}(\mathbf{r})\exp(-i\mathbf{Q}\cdot\mathbf{r})dr^3 \tag{2.3}$$

For magnetic scattering by a crystal, the vector field is the magnetic induction $\mathbf{B}(\mathbf{r}) = \mu_0\mathbf{H} + \mathbf{M}(\mathbf{r})$ where $\mathbf{H}$ is the applied magnetic field and $\mathbf{M}(\mathbf{r})$ is the magnetisation distribution in the crystal. The Q^{th} Fourier component is

$$\mathbf{M}_\perp(\mathbf{Q}) = \hat{\mathbf{Q}}\times\mathbf{F}_\mathbf{M}(\mathbf{Q})\times\hat{\mathbf{Q}} \tag{2.4}$$

with $\mathbf{F}_\mathbf{M}(\mathbf{Q}) = \int \mathbf{M}(\mathbf{r})\exp(-i\mathbf{Q}\cdot\mathbf{r})dr^3$.

$\hat{\mathbf{Q}}$ is a unit vector parallel to the scattering vector $\mathbf{Q}$.

$\mathbf{F}_\mathbf{M}(\mathbf{Q})$ is the *magnetic structure factor*, $\mathbf{M}_\perp(\mathbf{Q})$ is the *magnetic interaction vector*, both are in general complex vectors.

Eq.2.4 ensures that only components of magnetisation perpendicular to the scattering vector give rise to magnetic scattering.

2.2 Rotation of polarisation by magnetic scattering

In terms of the magnetic interaction vector the scattered intensity is proportional to

$$I = \mathbf{M}_\perp(\mathbf{Q})\cdot\mathbf{M}_\perp^*(\mathbf{Q}) - i\mathbf{P}\cdot\mathbf{M}_\perp(\mathbf{Q})\times\mathbf{M}_\perp^*(\mathbf{Q}) \tag{2.5}$$

and the scattered polarisation is given by

$$\begin{aligned}\mathbf{P}'I = {} & 2\Re(\mathbf{M}_\perp(\mathbf{Q})(\mathbf{P}\cdot\mathbf{M}_\perp^*(\mathbf{Q}))) + \mathbf{P}(\mathbf{M}_\perp(\mathbf{Q})\cdot\mathbf{M}_\perp^*(\mathbf{Q})) \\ & +i(\mathbf{M}_\perp(\mathbf{Q})\times\mathbf{M}_\perp^*(\mathbf{Q}))\end{aligned} \tag{2.6}$$

When $\mathbf{M}_\perp(\mathbf{Q})$ and $\mathbf{M}_\perp^*(\mathbf{Q})$ are parallel, the polarisation precesses by 180° about $\mathbf{M}_\perp(\mathbf{Q})$ as shown in Figure 1(a). When $\mathbf{M}_\perp(\mathbf{Q})$ and $\mathbf{M}_\perp^*(\mathbf{Q})$ are perpendicular, the scattered polarisation is perpendicular to both as in Figure 1(b).

2.3 Nuclear magnetic interference

Consider first just the nuclear scattering and assume that any nuclear spins are randomly oriented. Then the interaction between the neutron and the nucleus can be approximated by the Fermi pseudo potential

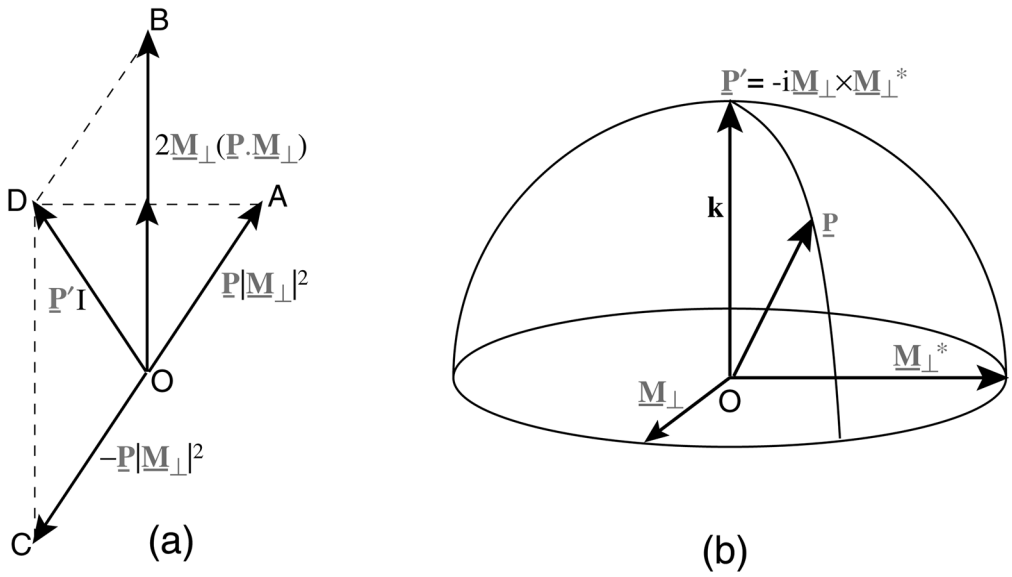

Figure 1. Rotation of the polarisation by pure magnetic scattering; (a) when $\mathbf{M}_\perp$ and $\mathbf{M}_\perp^*$ are parallel, (b) when $\mathbf{M}_\perp$ and $\mathbf{M}_\perp^*$ are perpendicular.

which is a scalar field. It is zero except very close to the nucleus. For this reason pure nuclear scattering (random nuclear spins) is independent of neutron polarisation.

$$\mathbf{P}'I = \mathbf{P}(F_N(\mathbf{Q})F_N^*(\mathbf{Q})) \quad \text{and} \quad I = F_N(\mathbf{Q})F_N^*(\mathbf{Q}) \tag{2.7}$$

$F_N(\mathbf{Q})$ is the *nuclear structure factor*, a complex scalar quantity. The coherent nuclear scattering does not alter the polarisation in either magnitude or direction. On the other hand, when magnetic and nuclear scattering occur in the same reflections (same $\mathbf{Q}$) their interference affects both the scattered intensity and the polarisation. The additional term in the intensity is

$$\mathbf{P} \cdot 2\Re(\mathbf{M}_\perp(\mathbf{Q})F_N^*(\mathbf{Q})) \tag{2.8}$$

It is proportional to the projection, in complex vector space, of $\mathbf{M}_\perp(\mathbf{Q})$ on $\mathbf{P}F_N(\mathbf{Q})$.

There are two additional terms in the polarisation, the first

$$2\Re(\mathbf{M}_\perp(\mathbf{Q})F_N^*(\mathbf{Q})) \tag{2.9}$$

is present only when the intensity is polarisation dependent as above. The second

$$\mathbf{P} \times 2\Im(\mathbf{M}_\perp(\mathbf{Q})F_N^*(\mathbf{Q})) \tag{2.10}$$

is only present if there is a component of $\mathbf{M}_\perp(\mathbf{Q})$, in complex vector space, which is perpendicular to $\mathbf{P}F_N(\mathbf{Q})$. This happens when $\mathbf{P}$ is not parallel to $\mathbf{M}_\perp(\mathbf{Q})$ and the phase difference between $\mathbf{M}_\perp(\mathbf{Q})$ and $F_N(\mathbf{Q})$ is neither 0 or 180°.

Nuclear magnetic interference can therefore change both the magnitude and direction of the polarisation. This is illustrated pictorially in Figure 2. In (a) both $\mathbf{M}_\perp(\mathbf{Q})$ and $F_N(\mathbf{Q})$ are real and the polarisation rotates in the plane containing $\mathbf{P}$ and $\mathbf{M}_\perp(\mathbf{Q})$. In (b) $\mathbf{M}_\perp(\mathbf{Q})$ and $F_N(\mathbf{Q})$ are in quadrature and the scattered polarisation is rotated towards $\mathbf{P} \times \mathbf{M}_\perp(\mathbf{Q})$.

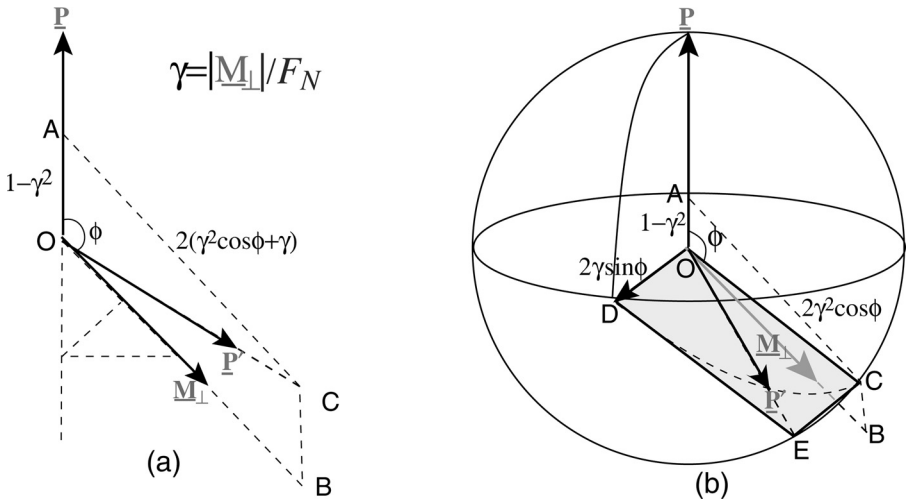

Figure 2. Rotation of the polarisation when magnetic and nuclear scattering occur together; (a) if both $\mathbf{M}_\perp(\mathbf{Q})$ and $F_N(\mathbf{Q})$ are real, (b) if $\mathbf{M}_\perp(\mathbf{Q})$ and $F_N(\mathbf{Q})$ are in quadrature.

2.4 The Blume Maleev equations

Combining the different contributions to the intensity and polarisation from Eqs.(2.5−2.10) leads to the Blume-Maleev equations [1,2]. These give the scattered intensity I and polarisation $\mathbf{P}'$ in terms of the incident polarisation $\mathbf{P}$.

$$\begin{aligned}
\mathbf{P}'I &= \mathbf{P}(|F_N|^2 - \mathbf{M}_\perp\cdot\mathbf{M}_\perp^*) && \text{part } \| \text{ to } \mathbf{P}\\
&\quad + 2\Re(\mathbf{M}_\perp(\mathbf{P}\cdot\mathbf{M}_\perp^*) + \mathbf{M}_\perp F_N^*) && \text{part } \| \text{ to } \mathbf{M}_\perp\\
&\quad + \mathbf{P}\times 2\Im(\mathbf{M}_\perp F_N^*) && \text{part } \perp \text{ to } \mathbf{P} \text{ and } \mathbf{M}_\perp\\
&\quad - \Im(\mathbf{M}_\perp\times\mathbf{M}_\perp^*) && \text{part } \| \text{ to } \mathbf{Q}\\
& && \text{zero if } \mathbf{M}_\perp \text{ is } \| \text{ to } \mathbf{M}_\perp^*\\
I &= |F_N|^2 + \mathbf{M}_\perp\cdot\mathbf{M}_\perp^* && \text{polarisation independent part}\\
&\quad + 2\Re(\mathbf{P}\cdot\mathbf{M}_\perp F_N^*) + \mathbf{P}\cdot\Im(\mathbf{M}_\perp\times\mathbf{M}_\perp^*) && \text{polarisation dependent part}
\end{aligned} \tag{2.11}$$

The polarisation is rotated in the scattering process whenever the magnetic interaction vector is not parallel to the incident polarisation.

2.5 Tensor representation of the scattered polarisation

The relationship between the incident and scattered polarisations can conveniently be described by a tensor equation.

$$\mathbf{P}' = \mathcal{P}\mathbf{P} + \mathbf{P}'' \quad \text{or in components} \quad \mathrm{P'}_i = \mathcal{P}_{ij}\mathrm{P}_j + \mathrm{P''}_i \tag{2.12}$$

$\mathbf{P}''$ is the polarisation created in the scattering process.

The unique direction defined by the scattering process is that of the scattering vector $\mathbf{Q}$. The experiment usually defines a second special direction: the normal to the scattering plane. It is therefore convenient to work with axes defined with respect to these directions:

1. x parallel to the crystallographic scattering vector $\boldsymbol{\kappa} = -\mathbf{Q}$
2. z normal to the scattering plane
3. y completing the right-handed orthogonal set

With this definition, there is no component of $\mathbf{M}_\perp(\mathbf{Q})$ parallel to x. These are the polarisation axes. The elements of $\mathcal{P}$ and $\mathbf{P}''$ can be written with respect to these axes as:

$$\begin{aligned}
\mathcal{P} &= \begin{pmatrix} (F_N^2 - M_\perp^2)/I_x & J_{nz}/I_x & J_{ny}/I_x \\ -J_{nz}/I_y & (F_N^2 - M_\perp^2 + R_{yy})/I_y & R_{yz}/I_y \\ -J_{ny}/I_z & R_{zy}/I_z & (F_N^2 - M_\perp^2 + R_{zz})/I_z \end{pmatrix} \\
\mathbf{P}'' &= \begin{pmatrix} -J_{yz}/I \\ R_{ny}/I \\ R_{nz}/I \end{pmatrix}
\end{aligned} \tag{2.13}$$

$$\begin{aligned}
I_x &= F_N^2 + M_\perp^2 + \mathrm{P}_x J_{yz} \\
I_y &= F_N^2 + M_\perp^2 + \mathrm{P}_y R_{ny} \\
I_z &= F_N^2 + M_\perp^2 + \mathrm{P}_z R_{nz} \\
I &= F_N^2 + M_\perp^2 + \mathrm{P}_x J_{yz} + \mathrm{P}_y R_{ny} + \mathrm{P}_z R_{nz}
\end{aligned} \tag{2.14}$$

$$\begin{aligned}
&F_N^2 = F_N(\mathbf{Q})F_N^*(\mathbf{Q}) && M_\perp^2 = \mathbf{M}_\perp(\mathbf{Q}) \cdot \mathbf{M}_\perp^*(\mathbf{Q}) \\
&R_{ij} = 2\Re(M_{\perp i}(\mathbf{Q})M_{\perp j}^*(\mathbf{Q})) && R_{ni} = 2\Re(F_N(\mathbf{Q})M_{\perp i}^*(\mathbf{Q})) \\
&J_{ij} = 2\Im(M_{\perp i}(\mathbf{Q})M_{\perp j}^*(\mathbf{Q})) && J_{ni} = 2\Im(F_N(\mathbf{Q})M_{\perp i}^*(\mathbf{Q}))
\end{aligned} \tag{2.15}$$

The off-diagonal components of $\mathcal{P}$ describe rotations of the polarisation.

3 SCATTERING FROM REAL CRYSTALS: MAGNETIC DOMAINS

The squared modulus of the scattered polarisation $|\mathbf{P}'|^2$ calculated from the Blume-Maleev equations is always greater than or equal to $|\mathbf{P}|^2$.

$$1 \geq |\mathbf{P}'|^2 \geq |\mathbf{P}|^2$$

The polarisation of the beam is therefore either increased or unchanged by scattering from a pure state.

Polarised beams scattered by real crystals are often at least partially depolarised. Such crystals contain a mixture of states usually corresponding to different magnetic domains. SNP can distinguish real depolarisation, due to a mixed state system, from rotation of the polarisation away from the incident direction because it can determine the off-diagonal elements of the polarisation matrix.

Magnetic domains will occur when the symmetry of the magnetic structure is less than that of the paramagnetic phase. If the order of the paramagnetic group is p and that of the magnetic group m; the number of different domains is p/m.

3.1 Configuration domains

Configuration domains exist whenever the propagation vector $\boldsymbol{\tau}$ describing the magnetic structure is not transformed either into itself, or itself plus a reciprocal lattice vector, by all the symmetry operators of the paramagnetic group. The operation of the paramagnetic symmetry on $\boldsymbol{\tau}$ generates a set of vectors which form the *star* of $\boldsymbol{\tau}$. Each distinct vector in the star generates a different configuration domain, and each configuration domain gives rise to a completely separate set of magnetic reflections as illustrated in Figure 3 for $\boldsymbol{\tau} = \frac{1}{2}\frac{1}{2}0$ and space group $P4/mmm$. Figure 3(a) shows the 4 arms of the star generated by the tetragonal symmetry, of which only 2 are independent since $2\boldsymbol{\tau}$ is a reciprocal lattice vector. Figure 3(b) gives the positions of the magnetic reflections in reciprocal space for both configuration domains.

Figure 4 shows the positions in reciprocal space of the magnetic reflections for each of the two configuration domains. These two domains correspond to different but equivalent propagation vectors $\boldsymbol{\tau}_1$ and $\boldsymbol{\tau}_2$. Each reflection belongs to a distinct configuration domain and hence effectively to a single state. For this reason configuration domains do not give rise to depolarisation.

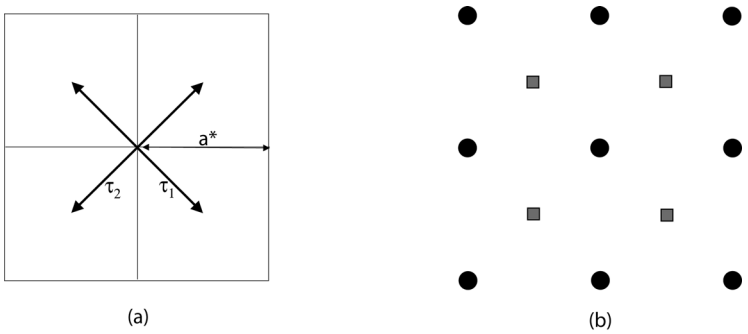

Figure 3. (a) The *star* of the propagation vector τ generated by tetragonal symmetry. (b) Positions in reciprocal space of the nuclear (circles) and magnetic (squares) reflections corresponding to the full star.

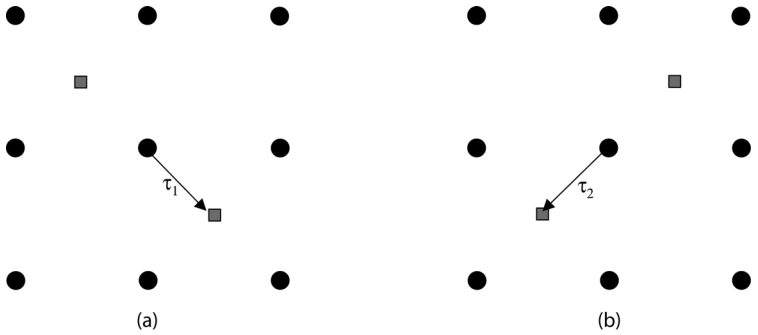

Figure 4. Positions in reciprocal space of magnetic reflections belonging to the two distinct configuration domains.

3.2 180° domains

180° degree domains are regions of crystal in which all the moment directions in one domain are reversed with respect to those in the other. $\mathbf{M}_\perp$ points in opposite directions in the two domains giving a phase difference of π between their scattering amplitudes. The two domains are related by the time inversion operator. Ferromagnetic domains provide a simple example of this type.

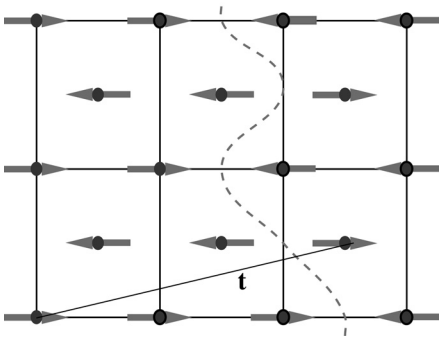

Figure 5. 180° domains in a face-centred lattice for a magnetic structure with $\boldsymbol{\tau} = 1, 0, 0$.

In a structure with non-zero propagation vector ($\boldsymbol{\tau} \neq 0$) the two 180° domains cannot be distinguished except by the defects associated with the domain walls. One domain can be transformed into the other by a translation $\mathbf{t}$ such that $\mathbf{t} \cdot \boldsymbol{\tau} = (2n + 1)/2$. The intensity and the polarisation scattered by the two domains are identical.

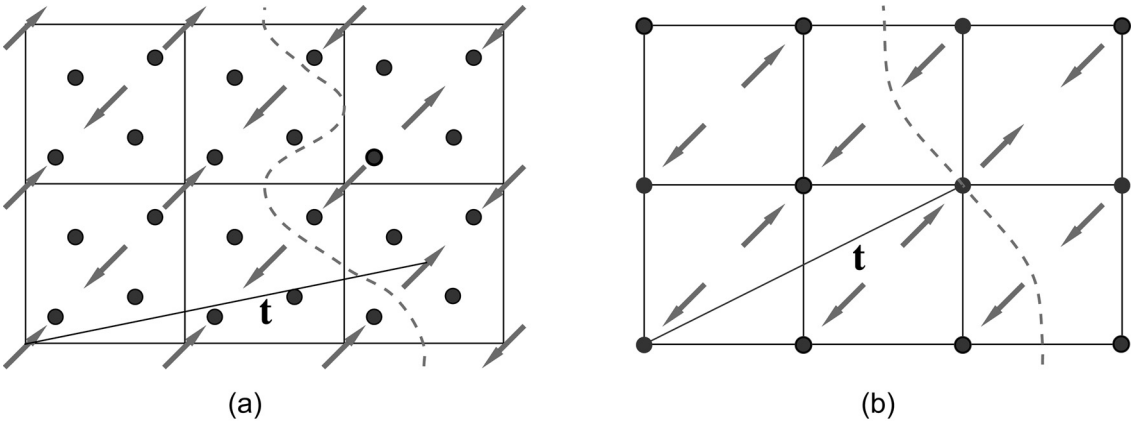

Figure 6. 180° domains in structures with $\boldsymbol{\tau}$= 0 (a) when the symmetry element which inverts the spin involves a *proper* rotation, (b) when it is an *improper* one ie involves an inversion.

When $\boldsymbol{\tau} = 0$, a rotation as well as a translation is needed to transform one 180° domain into the other. Figure 6(a) shows an example of a centrosymmetric structure in which oppositely oriented moments are related by a rotation of $\pi/2$ and a translation of $(\frac{1}{2}\frac{1}{2}0)$. Both magnetic and nuclear structure factors are real so that the terms R_{ni} in Eq.2.13 are non-zero. They could lead to a polarisation dependent cross-section, and increase the polarisation parallel to $\mathbf{M}_\perp$. However these terms have opposite signs for the two domains and if they are equally populated R_{ni} will average to zero. There is no depolarisation due to this type of 180° domain.

Figure 6(b) shows the case of a centrosymmetric structure in which oppositely oriented moments are related by a centre of symmetry. In this case the magnetic and nuclear scattering are in quadrature. The terms J_{ni} in Eq.2.13 are finite, they induce a rotation of the polarisation towards the direction perpendicular to both $\mathbf{M}_\perp$ and $\mathbf{P}$. They too have opposite signs for the two domains and, in a mixed domain crystal, will lead to some depolarisation unless the incident polarisation is parallel to $\mathbf{M}_\perp$.

3.3 Orientation domains (s-domains)

Orientation domains occur when the magnetic space group is not congruent with the group describing the configurational symmetry. If $\mathcal{P}$ is a sub-group of the configurational symmetry $\mathcal{G}$, congruent with the magnetic space group $\mathcal{M}$, the orientation domains are generated by the subgroup $\mathcal{S}$ of $\mathcal{G}$ made up of operators contained in $\mathcal{G}$ which are not in the magnetic group. $\mathcal{S}$ is such that

$$\mathcal{G} = \mathcal{P} \times \mathcal{S}.$$

If $\mathcal{S}$ is of order s then there are s possible orientation domains related to one another by the elements of $\mathcal{S}$. The magnetic interaction vectors for reflections related by these elements are different.

$$\mathbf{M}_\perp(\mathbf{Q}) \neq \mathbf{M}_\perp(\tilde{\mathbf{R}}_s\mathbf{Q}) \quad \text{but} \quad \mathbf{M}_{\perp s}(\mathbf{Q}) = \mathbf{M}_\perp(\tilde{\mathbf{R}}_s\mathbf{Q}) \tag{3.1}$$

Where $\tilde{\mathbf{R}}_s$ is an operator in $\mathcal{S}$ and $\mathbf{M}_{\perp s}(\mathbf{Q})$ is the interaction vector for the domain generated by $\tilde{\mathbf{R}}_s$. For collinear structures, the magnetic structure factors of reflections related by the elements of $\mathcal{S}$ are equal:

$$\tilde{\mathbf{R}}_s\mathbf{F}_\mathbf{M}(\mathbf{Q}) = \mathbf{F}_\mathbf{M}(\tilde{\mathbf{R}}_s\mathbf{Q})$$

but this is not true in the general case.

If the configurational symmetry possesses a symmetry axis of order higher than 2 then either the moments lie parallel to this axis, or the structure is non collinear, or the symmetry axis is not in the magnetic space group. Equally, in a collinear structure, either the moments lie parallel to any mirror

planes and diad axes, or they are perpendicular to them, or the mirror plane or diad axis is not in the magnetic space group.

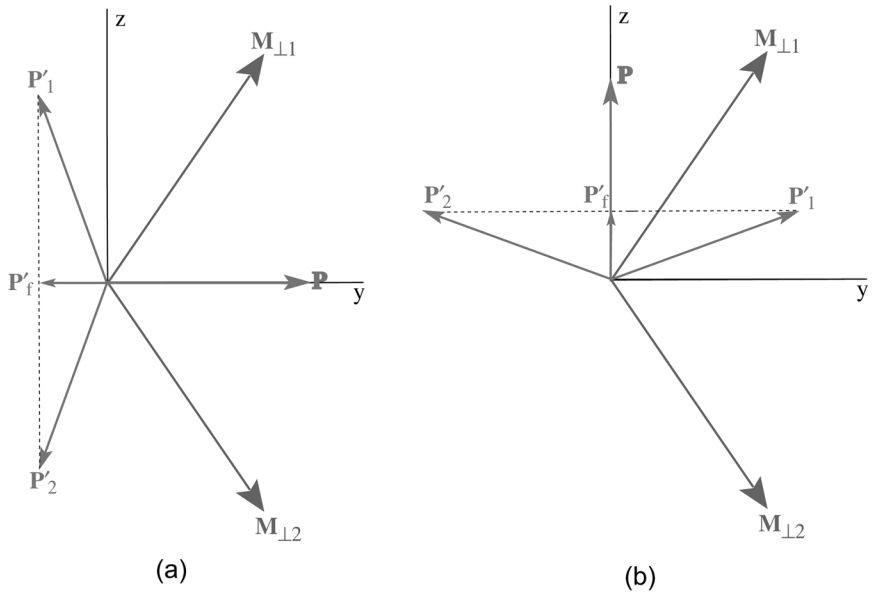

Figure 7. Rotation of the scattered polarisation by orientation domains (a) s-domains related by a diad axis parallel to y; (b) s-domains related by a mirror plane perpendicular to z

Figure 7 illustrates how the presence of s-domains may depolarise the beam. In Figure 7(a) the domains 1 and 2 and their interaction vectors $\mathbf{M}_{\perp 1}$ and $\mathbf{M}_{\perp 2}$ are related by a diad axis parallel to y. $\mathbf{P'}_1$ and $\mathbf{P'}_2$ are the directions of the polarisation scattered by the two domains when $\mathbf{P}$ is parallel to y; they have opposite z components. In an equi-domain crystal only the components of scattered polarisation parallel to y (and x) are preserved. In Figure 7(b) domains 1 and 2 and their interaction vectors $\mathbf{M}_{\perp 1}$ and $\mathbf{M}_{\perp 2}$ are related by a mirror plane parallel to z. In this case only the components of scattered polarisation parallel to z (and x) will be preserved if the domain populations are equal. In this way orientation domains can give rise to depolarisation of the y and z components of polarisation; the x component is never depolarised. The directions for which depolarisation occurs can help to identify the missing symmetry elements.

3.4 Chirality domains

Chirality domains can occur whenever the paramagnetic space group is centrosymmetric but the magnetic structure is not. They are related by the inversion operator. This happens either when the magnetic moments on centrosymmetrically related sites are not parallel or when $2\boldsymbol{\tau}$ is not a reciprocal lattice vector so the configurational group is acentric. In this latter case the two chirality domains correspond to + and – $\boldsymbol{\tau}$. They both give reflections at $\mathbf{g} \pm \boldsymbol{\tau}$ with

$$\mathbf{M}_{\perp\boldsymbol{\tau}}(\mathbf{g}+\boldsymbol{\tau}) = -\mathbf{M}^{*}_{\perp\boldsymbol{\tau}}(\mathbf{g}-\boldsymbol{\tau}) = -\mathbf{M}^{*}_{\perp -\boldsymbol{\tau}}(g+\boldsymbol{\tau}) \tag{3.2}$$

Such structures include helices and cycloids.

In chiral structures, $\mathbf{M}_{\perp}(\mathbf{Q})$ is not parallel to $\mathbf{M}^{*}_{\perp}(\mathbf{Q})$ so the J_{ij} terms in the polarisation matrix are non-zero, they have opposite signs for the two chiralities. Chirality domains do not lead to depolarisation but if they are unequally populated the polarisation parallel to x can increase and the intensity will be polarisation dependent.

4 MAGNETIC STRUCTURE DETERMINATION USING SNP

4.1 Experimental strategies

SNP cannot be used in isolation to determine magnetic structure.

- The magnetic propagation vector $\boldsymbol{\tau}$ must be known.
- If $\boldsymbol{\tau} \neq 0$, intensity measurements are needed to determine the absolute magnitudes of the moments.
- With the current SNP geometry, $\boldsymbol{\tau}$ must be set in the scattering plane.
- It is advantageous to orient the crystal so that a component of magnetisation is perpendicular to the scattering plane.
- Analysis of rather few magnetic reflections is then usually sufficient to determine the structure.

The usual experimental strategy is to measure the scattered polarisation $\mathbf{P}'$ with the incident polarisation $\mathbf{P}$ parallel to polarisation x, y, z in turn. This determines the polarisation matrix. The *polarisation matrix* P is an experimental quantity related to the polarisation tensor. The matrix element P_{ij} gives the j^{th} component of scattered polarisation when the incident polarisation is in the i^{th} direction.

$$\mathsf{P}_{ij} = \left\langle \frac{\mathrm{P}_i \mathcal{P}_{ij} + \mathrm{P''}_j}{\mathrm{P}_i} \right\rangle_{\text{domains}} \tag{4.1}$$

4.2 Commensurate structures with non-zero propagation vectors

For structures with $\boldsymbol{\tau} = 0$, $F_N(\mathbf{Q})$ is zero at the positions of magnetic reflections. So the terms R_{ny}, R_{nz}, J_{ny} and J_{nz} in the polarisation tensor are all zero. If the magnetic space-group is centrosymmetric, J_{yz} is also zero, so $\mathbf{P''}$= 0. The phases can be chosen to make $\mathbf{M}_\perp(\mathbf{Q})$ real and if it is inclined at an angle α to z (measured clockwise about x), the polarisation tensor has the simple form:

$$\mathcal{P} = \begin{pmatrix} -1 & 0 & 0 \\ 0 & -\cos 2\alpha & -\sin 2\alpha \\ 0 & -\sin 2\alpha & \cos 2\alpha \end{pmatrix} \tag{4.2}$$

If $\mathbf{M}_\perp(\mathbf{Q})$ is parallel to either y or z, the matrix is diagonal.

$$\begin{array}{lll} (a) & \mathbf{M}_\perp \parallel y) & \\ \mathcal{P} & = & \begin{pmatrix} -1 & 0 & 0 \\ 0 & 1 & 0 \\ 0 & 0 & -1 \end{pmatrix} \end{array} \qquad \begin{array}{lll} (b) & \mathbf{M}_\perp \parallel z & \\ \mathcal{P} & = & \begin{pmatrix} -1 & 0 & 0 \\ 0 & -1 & 0 \\ 0 & 0 & 1 \end{pmatrix} \end{array} \tag{4.3}$$

When s-domains with different directions of $\mathbf{M}_\perp(\mathbf{Q})$ are present, the off-diagonal elements P_{yz} and P_{zy} are reduced and the scattered beam is partly depolarised when $\mathbf{P}$ is not parallel to x.

The value of SNP for commensurate magnetic structures is its ability to uniquely determine the orientation of $\mathbf{M}_\perp(\mathbf{Q})$.

The commensurate structure of cupric oxide

The commensurate structure of cupric oxide provides a simple example.

- Below 213 K, cupric oxide CuO (space group C2/c) has a commensurate antiferromagnetic structure with $\boldsymbol{\tau} = \frac{1}{2}, 0, -\frac{1}{2}$.
- Magnetic reflections $h0l \pm \boldsymbol{\tau}$, with $h + l$ odd, are systematically absent showing that the spins on copper atoms, related by the n glide-plane perpendicular to **b**, are parallel.
- The reflection intensities suggest that the spin-direction is **b** [3].

SNP measurements were undertaken to confirm this structure [5].

The crystal was aligned with [010] perpendicular to the scattering plane so that the $h0l$ reflections could be measured. The polarisation matrices measured for the $\frac{1}{2},0,\frac{1}{2}$ $\bar{\frac{1}{2}},0,\frac{1}{2}$ $\frac{3}{2},0,\bar{\frac{3}{2}}$ and $\frac{3}{2},0,\frac{1}{2}$ reflections were identical within experimental error, they all had the diagonal form of Eq.4.3(b). This shows conclusively that the structure must be collinear with spins parallel to polarisation $z = [010]$ as shown in Figure 8.

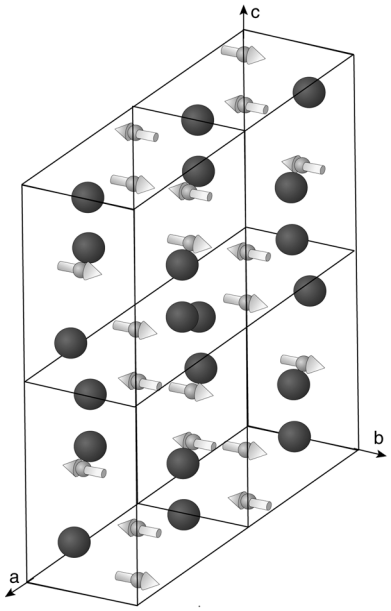

Figure 8. Magnetic structure of the commensurate phase of CuO.

Choosing between canted and collinear models

To show how SNP can distinguish between canted and collinear structures, a tetragonal structure with propagation vector $\boldsymbol{\tau} = 0,0,\frac{1}{2}$ is used as an example. There are 4 magnetic atoms per cell: A1 at $(x,x,0)$; A2 at $(-x,x,0)$, A3 at $(-x,-x,0)$; A4 at $(x,-x,0)$ with $x \approx 0.2$. The spins lie in the 001 plane.

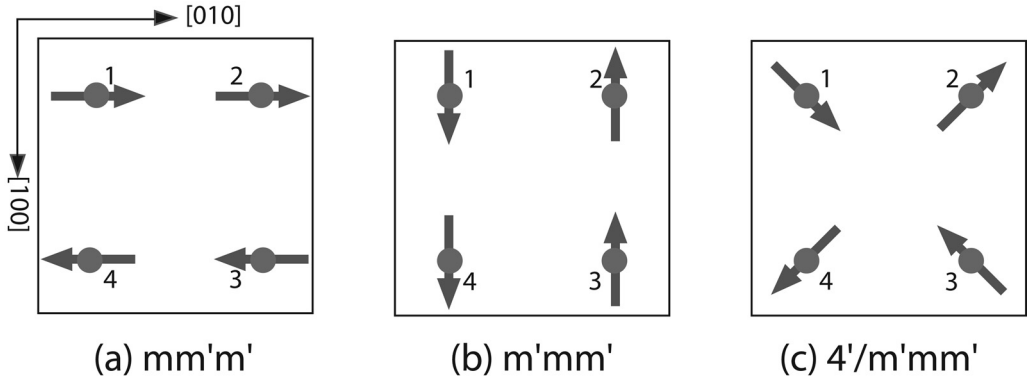

Figure 9. The $z = 0$ plane for three possible spin configurations of a tetragonal structure with $\boldsymbol{\tau}$ = 0,0,$\frac{1}{2}$.

Possible configurations of the plane at $z = 0$ are shown in Figure 9. The form of the magnetic structure factors for the three models is given in Table 1, from which it can be seen that:

- The average intensity scattered by the two orthorhombic domains is exactly the same as that scattered by the tetragonal structure.
- The tetragonal structure gives a unique $\mathbf{F_M(Q)}$ for each reflection. SNP can determine its direction.
- A mixture of orthorhombic domains will give depolarisation for **P** perpendicular to **Q** because the structure factors for the two domains are not parallel.

Table 1. Components of the magnetic structure factors $\mathbf{F_M(Q)}$ for hkl reflections.

Component	Model (a)	Model (b)	Model (c)
$M_{[100]}$	0	$4Ss(h)c(k)$	$2\sqrt{2}Ss(h)c(k)$
$M_{[010]}$	$4Ss(k)c(h)$	0	$2\sqrt{2}Ss(k)c(h)$
Intensity	$(4Ss(k)c(h))^2$	$(4Ss(h)c(k))^2$	$8S^2(s^2(h)c^2(k)+s^2(k)c^2(h))$
Domain Average	$8S^2(s^2(h)c^2(k)+s^2(k)c^2(h))$		

$c(h) = \cos 2\pi hx$; $s(h) = \sin 2\pi hx$ $c(k) = \cos 2\pi kx$; $s(k) = \sin 2\pi kx$

Table 2. Components of the magnetic interaction vectors $\mathbf{M}_\perp\mathbf{(Q)}$ for $0kl$ reflections.

Component	Model (a)	Model (b)	Model (c)	Notes
$M_{\perp y}$	0	$2F'\sin\alpha$	$\sqrt{2}F'\sin\alpha$	$F = S\sin 2\pi hx$
$M_{\perp z}$	$2F$	0	$\sqrt{2}F$	$F' = S\cos 2\pi hx$
Magnetic Intensity	$4F^2$	$4F'^2\sin^2\alpha$	$2(F^2+F'^2\sin^2\alpha)$	$I = F^2+F'^2\sin^2\alpha$

In an SNP experiment, to distinguish the models, the crystal would be mounted so as to have the $h, 0, \frac{1}{2}+l$ reflections in the scattering plane: [010] parallel to polarisation z. The components $M_{\perp y}$, $M_{\perp x}$ of the magnetic interaction vectors for the different models are given in Table 2 for a reflection $h0l$ whose scattering vector is inclined at an angle α to [100].

The corresponding polarisation matrices are:

Model (a)

$$\mathbf{P} = \begin{pmatrix} -1 & 0 & 0 \\ 0 & -1 & 0 \\ 0 & 0 & 1 \end{pmatrix}$$

Model (b)

$$\mathbf{P} = \begin{pmatrix} -1 & 0 & 0 \\ 0 & 1 & 0 \\ 0 & 0 & -1 \end{pmatrix}$$

Model (c)

$$\mathbf{P} = \begin{pmatrix} -1 & 0 & 0 \\ 0 & -(F'^2 - F^2\sin^2\alpha)/I & (2FF'\sin\alpha)/I \\ 0 & (2FF'\sin\alpha)/I & (F'^2 - F^2\sin^2\alpha)/I \end{pmatrix}$$

The mean from equal volumes of domains (a) and (b) is

$$\mathbf{P} = \begin{pmatrix} -1 & 0 & 0 \\ 0 & -(F'^2 - F^2\sin^2\alpha)/I & 0 \\ 0 & 0 & (F'^2 - F^2\sin^2\alpha)/I \end{pmatrix}$$

Only the off-diagonal terms differ. They could be measured in an SNP experiment.

4.3 Incommensurate structures

SNP has been used rather successfully in determining the details of incommensurate structures such as helices, cycloids and spin-density waves. It also often allows these types of structures to be distinguished.

To study incommensurate structures some thought must be given to the crystal orientation.

- The propagation vector must lie in the scattering plane.
- A component of moment should be perpendicular to the scattering plane. If both components of the moment lie in the scattering plane, then $\mathbf{M}_\perp$ is parallel to polarisation y for all the accessible reflections. When $\boldsymbol{\tau} \neq 0$, it is only the direction and not the magnitude of $\mathbf{M}_\perp$ which is measured by SNP, so measuring different reflections in the zone gives no additional information.
- If the orientation is chosen so that a component of moment is parallel to polarisation z then the full potential of SNP can be realised.

The magnetic moment distribution in a sinusoidally modulated structure with lattice vectors $\boldsymbol{l}$ and propagation vector $\boldsymbol{\tau}$ can be written as

$$\mathbf{M}(\mathbf{r}+\boldsymbol{l}) = \hat{\mathbf{p}} M_p(\mathbf{r}) \cos \boldsymbol{l}\cdot\boldsymbol{\tau} + \hat{\mathbf{q}} M_q(\mathbf{r}) \sin \boldsymbol{l}\cdot\boldsymbol{\tau} \tag{4.4}$$

where $\hat{\mathbf{p}}$ and $\hat{\mathbf{q}}$ are perpendicular unit vectors.

- When either $M_p(\mathbf{r})$ or $M_q(\mathbf{r})$ is zero, modul describes a spin-density wave.
- When $\boldsymbol{\tau}$ lies in the plane of $\hat{\mathbf{p}}$ and $\hat{\mathbf{q}}$, it describes a cycloid.
- When both are perpendicular to $\boldsymbol{\tau}$ it describes a right helix.

The magnetic scattering from such a modulated structure is given by

$$\begin{aligned}\mathbf{M}_\perp(\mathbf{Q}) = &(\mathbf{p}_\perp M_p(\mathbf{Q}) - \imath\mathbf{q}_\perp M_q(\mathbf{Q}))\delta(\mathbf{g}+\boldsymbol{\tau}-\mathbf{Q}) \\ &+(\mathbf{p}_\perp M_p(\mathbf{Q}) + \imath\mathbf{q}_\perp M_q(\mathbf{Q}))\delta(\mathbf{g}-\boldsymbol{\tau}-\mathbf{Q})\end{aligned}$$

where $\mathbf{p}_\perp$ and $\mathbf{q}_\perp$ are the components of $\hat{\mathbf{p}}$ and $\hat{\mathbf{q}}$ perpendicular to $\mathbf{Q}$.

$$M_{p,q}(\mathbf{Q}) = \int_{\text{unit cell}} M_{p,q}(\mathbf{r}) exp - (\mathbf{Q}.\mathbf{r}) dr^3 \tag{4.5}$$

are the unit cell structure factors for the two perpendicular magnetic moment distributions.

- A structure with propagation vector $\boldsymbol{\tau}$ gives reflections at **both** $\mathbf{g}+\boldsymbol{\tau}$ **and** $\mathbf{g}-\boldsymbol{\tau}$.
- For structures for which $M_{p,q}(\mathbf{Q})$ are real, ie the magnetisation distributions themselves are centrosymmetric $\mathbf{M}_\perp(\mathbf{Q})_{\boldsymbol{\tau}} = \mathbf{M}^*_\perp(\mathbf{Q})_{-\boldsymbol{\tau}}$.
- The term in the polarisation matrix which creates polarisation along x: $J_{ij} = 2\Re(M_p(\mathbf{Q})M_q(\mathbf{Q}))|\mathbf{p}_\perp \times \mathbf{q}_\perp|$ is finite if neither $\mathbf{p}_\perp$, $\mathbf{q}_\perp$ or either structure factor $M_{p,q}(\mathbf{Q})$ is zero.

An example will show how SNP measurements determine the structure when $M_{p,q}(\mathbf{Q})$ are real. The crystal must be aligned with $\boldsymbol{\tau}$ in the scattering plane. Suppose for simplicity that $\hat{\mathbf{p}}$ is perpendicular to the scattering plane so that $\hat{\mathbf{q}}$ lies in it. For the different reflections in the scattering plane, $\mathbf{p}_\perp \parallel z$ is constant, whilst $\mathbf{q}_\perp \parallel y$ varies from 0 when $\hat{\mathbf{q}} \parallel \mathbf{Q}$ to a maximum when $\hat{\mathbf{q}} \perp \mathbf{Q}$.

The polarisation matrices which would be obtained are:

$$\mathbf{P} = \begin{pmatrix} -1 & 0 & 0 \\ B & A & 0 \\ B & 0 & -A \end{pmatrix} \quad \text{for} \quad \mathbf{Q} \parallel \hat{\mathbf{q}} \quad \text{with} \quad A = \tfrac{M_p(\mathbf{Q})^2 - M_q(\mathbf{Q})^2}{M_p(\mathbf{Q})^2 + M_q(\mathbf{Q})^2}$$

$$\mathbf{P} = \begin{pmatrix} -1 & 0 & 0 \\ 0 & -1 & 0 \\ 0 & 0 & 1 \end{pmatrix} \quad \text{for} \quad \mathbf{Q} \perp \hat{\mathbf{q}} \quad \text{and} \quad B = \frac{2M_p(\mathbf{Q})M_q(\mathbf{Q})}{M_p(\mathbf{Q})^2 + M_q(\mathbf{Q})^2}$$

$$\mathbf{P} = \begin{pmatrix} -1 & 0 & 0 \\ -B & A & 0 \\ -B & 0 & -A \end{pmatrix} \quad \text{for} \quad \mathbf{Q} \parallel \hat{\mathbf{q}} \quad \text{for the other chirality domain}$$

Points to note are that:

- $\mathsf{P}_{xx} = -1$ in all three cases; in fact this must always be so when $\boldsymbol{\tau} \neq 0$.
- For $\mathbf{P} \perp \mathbf{Q}$, there is no y component of $\mathbf{M}_\perp(\mathbf{Q})$ and so the behaviour is the same as for a collinear structure with $\mathbf{M}_\perp(\mathbf{Q}) \parallel \mathbf{z}$.
- For $\mathbf{P} \parallel \mathbf{Q}$, the P_{yy} and P_{zz} components give the ellipticity of the helix. They will be zero if the envelope is circular. The intensity scattered by the domain for which B is positive will be greater than that for which B is negative.
- The components P_{yx} and P_{zx} have opposite signs for the two chirality domains and if the two are equally populated will average to zero leading to a diagonal polarisation matrix.

The incommensurate structure of cupric oxide

At its Néel temperature, 230 K, CuO orders magnetically with an incommensurate structure $\boldsymbol{\tau}$= 0.506, 0, –0.483 which remains constant on further cooling down to a lock-in transition at 213 K. The systematically absent magnetic reflections follow the same rules as in the low temperature phase (section 4.2). This suggests that the coupling between moments in the two phases is nearly the same. Integrated intensity measurements were not able to distinguish clearly between different possible models for the modulation [3]. SNP measurements of a few $h0l \pm \boldsymbol{\tau}$ reflections were able to resolve the problem [4].

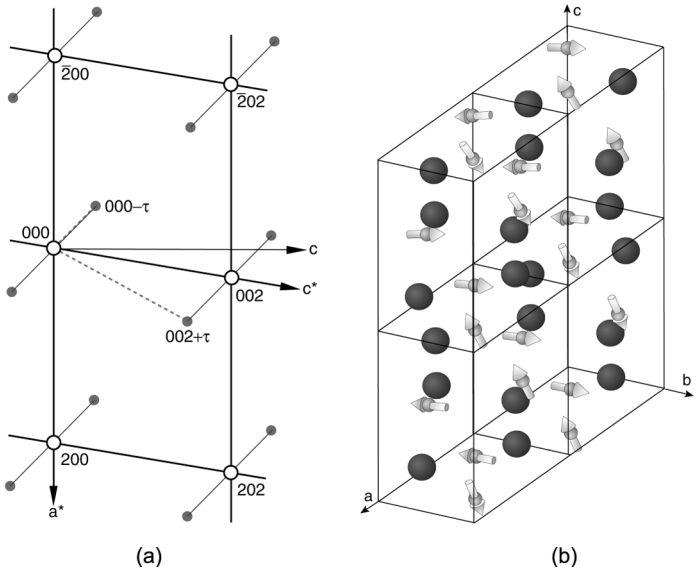

Figure 10. (a) The $h0l$ layer of the CuO reciprocal lattice, showing the positions of magnetic reflections of the incommensurate phase. (b) The incommensurate magnetic structure of CuO.

The scattering vectors for the $002 + \boldsymbol{\tau}$ and $000 - \boldsymbol{\tau}$ reflections are nearly perpendicular. The polarisation matrix for $002 + \boldsymbol{\tau}$ was similar to those measured in the commensurate phase. Therefore for $002 + \boldsymbol{\tau}$, $\mathbf{M}_\perp$ is parallel to [010]. The matrix obtained for $000 - \boldsymbol{\tau}$ was very different.

$$\mathbf{P}(000-\boldsymbol{\tau}) = \begin{pmatrix} -1.00 & 0.00 & -0.04 \\ -0.08 & -0.07 & 0.00 \\ -0.08 & 0.00 & 0.06 \end{pmatrix}$$

- The full polarisation is only transmitted for the x direction.
- The small values of P_{xy} and P_{xz} are due to cancellation of the off-diagonal elements from opposite chirality domains.
- The small values of P_{yy} and P_{zz} show that for this reflection $M_{\perp p}$ and $M_{\perp q}$ are nearly equal.

These results are only consistent with the helical structure shown in Figure 10(b) in which the spins rotate in a plane containing the $\mathbf{b}$ axis and the normal to $002+\boldsymbol{\tau}$.

Magnetic structure of UPtGe

The orthorhombic intermetallic compound UPtGe was reported to order magnetically at 51 K to a cycloidal structure with propagation vector $\boldsymbol{\tau} = 0, 0.554, 0$ with U spins rotating in the $\mathbf{b}-\mathbf{c}$ plane as shown in Figure 11(a) [6]. The plausibility of such a structure was queried because of the huge magnetic anisotropy found for U in other UTX compounds.

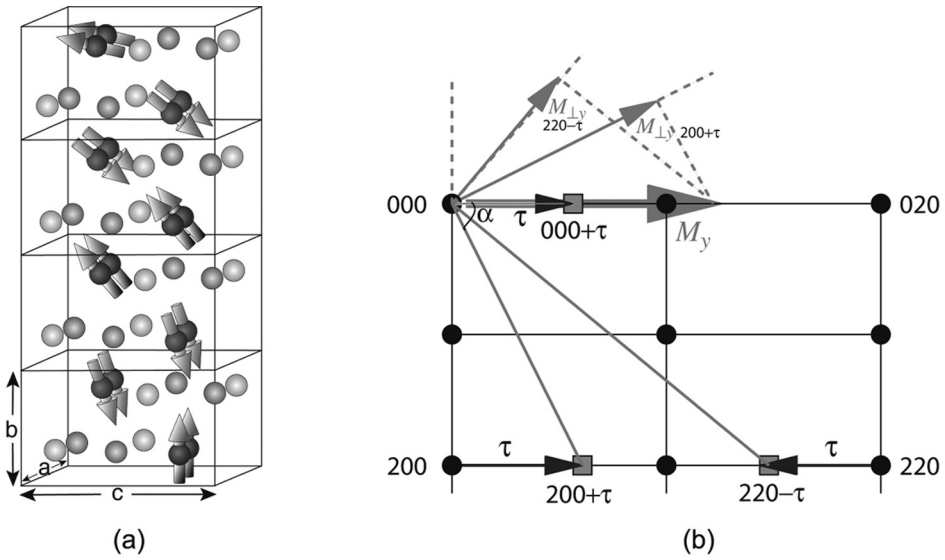

Figure 11. (a) The cycloidal magnetic structure of UPtGe and (b) the $hk0$ plane of the corresponding reciprocal lattice.

The proposed structure was verified by measuring the polarisation matrices for the reflections in the $hk0$ plane shown in Figure 11(b) with the following results:

$$\mathbf{P}(000+\tau) = \begin{pmatrix} -0.98 & 0.00 & 0.00 \\ 0.00 & -0.99 & 0.00 \\ 0.00 & 0.00 & 1.00 \end{pmatrix}$$

shows $\mathbf{M}_{\perp} \parallel z$

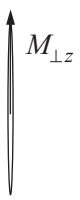

$$\mathbf{P}(200+\tau)=\begin{pmatrix}0.50 & 0.00 & 0.00\\ 1.02 & 0.00 & 0.00\\ 1.02 & 0.02 & 0.04\end{pmatrix}$$

gives $\mathbf{P'}\|-x$ for all $\mathbf{P}$

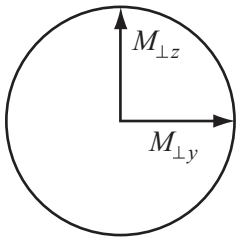

With $\mathbf{P}\| \; x$, the scattered intensity was very small and P_{xx} poorly determined.

$$\mathbf{P}(220-\tau)=\begin{pmatrix}-0.98 & 0.05 & -0.05\\ -0.98 & -0.10 & -0.02\\ -0.98 & 0.01 & 0.17\end{pmatrix}$$

$\mathbf{P'}\|-x$ with small P_{zz}

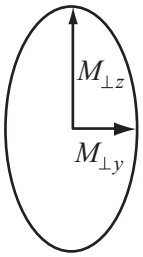

These results are characteristic of a nearly single domain cycloid structure in which the populated domain has $\boldsymbol{\tau} \parallel -x$ [7].

The ellipticity of the envelope $\epsilon = \frac{M_{[010]}}{M_{[001]}} = \frac{\text{major}}{\text{minor}}$ axes and the orientation of the major axis of the cycloid was obtained by fitting

$$\mathsf{P}_{yy}(\mathbf{Q}) = -\mathsf{P}_{zz}(\mathbf{Q}) = \pm\frac{\epsilon^2\sin^2\phi_{\mathbf{Q}}-1}{\epsilon^2\sin^2\phi_{\mathbf{Q}}+1}$$

for a set of magnetic reflections; $\phi_{\mathbf{Q}}$ is the angle between the major axis and $\mathbf{Q}$.

4.4 Magnetic structures with zero propagation vector

As was pointed out in section 2.3, when the magnetic propagation vector is zero, magnetic and nuclear scattering can occur in the same reflections. The terms

$$J_{ni} = 2\Im(F_N(\mathbf{Q})M^*_{\perp i}(\mathbf{Q})) \quad \text{and} \quad R_{ni} = 2\Re(F_N(\mathbf{Q})M^*_{\perp i}(\mathbf{Q}))$$

in the polarisation matrix (Eq.2.13 and Eq.2.14) can be non-zero. Finite R_{ni} results in a polarisation dependent cross-section. The scattered beam is polarised parallel to $\mathbf{M}_\perp$. This occurs when the phase angle between $\mathbf{M}_\perp(\mathbf{Q})$ and $F_N(\mathbf{Q}) \neq (2n+1)\pi$. It is the term used to determine magnetic structure factors from *flipping ratios*. Finite J_{ni} leads to rotation of the scattered polarisation towards a direction perpendicular to both $\mathbf{M}_\perp$ and $\mathbf{P}$. This occurs when the phase angle between $\mathbf{M}_\perp(\mathbf{Q})$ and $F_N(\mathbf{Q}) \neq 2n\pi$.

Resolving homometry in the RE manganites

The manganites $RMnO_3$ of the smaller rare-earth ions (R = Y, Ho, Er, Tm, Yb, Lu) crystalise with an hexagonal structure [8]. The manganese occupy sites $(x,0,0)$ with $x \approx 1/3$. They order magnetically below about 80 K with their moments in the (001) plane forming a triangular array. Alternative arrangements with different symmetries which have been proposed are shown in Figure 12.

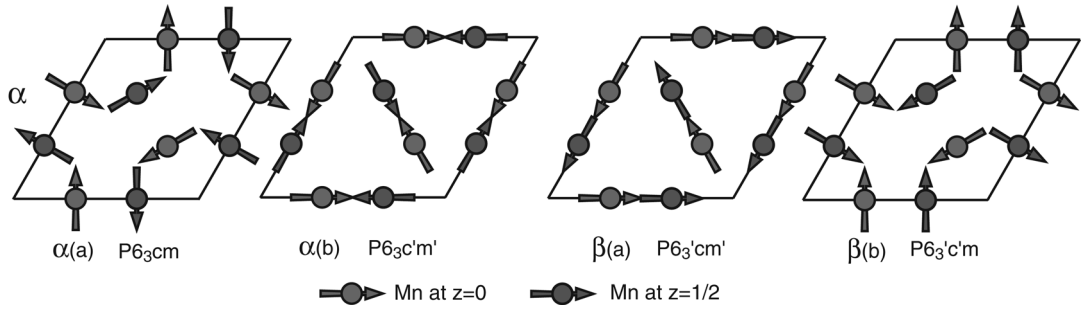

Figure 12. [001] projections showing possible spin configurations for the rare earth manganites.

Table 3. Contributions of manganese moments to the components of the magnetic interaction vectors of $h0l$ reflections for different ordering models of rare earth manganites.

Model	Parity	$M_{\perp y}$	$M_{\perp z}$
$\alpha(a)$	l odd	$(G-1)\cos\alpha$	0
	l even	0	$\imath\sqrt{3}G'$
$\beta(a)$	l odd	$\imath\sqrt{3}G'\cos\alpha$	0
	l even	0	$1-G$
$\alpha(b)$	l odd	0	$1-G$
	l even	$\imath\sqrt{3}G'\cos\alpha$	0
$\beta(b)$	l odd	0	$\imath\sqrt{3}G'$
	l even	$(G-1)\cos\alpha$	0

When $x_{\mathrm{Mn}} = \frac{1}{3}$, $\quad |1-G|^2 = 3|G'|^2$ for all h

$$\begin{aligned} G &= \cos 2\pi h x_{\mathrm{Mn}} \\ G' &= \sin 2\pi h x_{\mathrm{Mn}} \\ \alpha &= \tan^{-1}\sqrt{3}la/2hc \end{aligned}$$

The magnetic structures have never been completely resolved. The a and b structures of Figure 12 can be distinguished by intensity measurements, but if $x = 1/3$, the magnetic intensities for the α and β pairs are exactly the same [9]. Since x is not exactly 1/3, this homometry is not exact but the intensities are not sufficiently different to permit distinction between the α and β types. In $YMnO_3$, intensity measurements show that the structure is of the b type. In $HoMnO_3$, a transition from the a to b type takes place around 37 K.

Table 3 shows that whilst the intensities of the magnetic reflections are almost the same for the α and β models, their phases are very different and consequently the nuclear-magnetic interference terms differ widely. SNP therefore offers the possibility of a direct solution to the homometry by exploiting the directional and phase sensitivity of polarisation analysis.

Since the structure is non-centrosymmetric, the nuclear structure factors are complex. They can be written in terms of a modulus N and a phase angle ϕ as

$$F_N(\mathbf{Q}) = N(\mathbf{Q})\cos\phi + \imath N(\mathbf{Q})\sin\phi$$

The 180° domain imbalance in the crystal can be defined by a domain fraction η

$$\eta = \frac{v_1 - v_2}{v_1 + v_2} \tag{4.6}$$

where v_1 and v_2 are the volumes of crystal belonging to each of the two domains. The polarisation matrices which would be measured for the $h0l$ reflections are given in terms of η and the nuclear and magnetic structure factors in Table 4. So long as $\eta \neq 0$, the distinction between the models is clear. Unfortunately, it seems to be difficult to unbalance the domain populations and so, as yet, this method has not resolved the structures.

Table 4. Polarisation matrices of $h0l$ reflections calculated for the different magnetic structure models for $YMnO_3$.

Model	h0l with l odd **P**	h0l with l even **P**
$\alpha(a)$	$\begin{pmatrix} \beta & 0 & \eta\xi\sin\phi \\ \eta\xi\cos\phi & 1 & \eta\xi\cos\phi \\ -\eta\xi\sin\phi & 0 & \beta \end{pmatrix}$	$\begin{pmatrix} \beta & \eta\xi\cos\phi & 0 \\ -\eta\xi\cos\phi & \beta & 0 \\ \eta\xi\sin\phi & \eta\xi\sin\phi & 1 \end{pmatrix}$
$\beta(a)$	$\begin{pmatrix} \beta & 0 & \eta\xi\cos\phi \\ \eta\xi\sin\phi & 1 & \eta\xi\sin\phi \\ -\eta\xi\cos\phi & 0 & \beta \end{pmatrix}$	$\begin{pmatrix} \beta & \eta\xi\sin\phi & 0 \\ -\eta\xi\sin\phi & \beta & 0 \\ \eta\xi\cos\phi & \eta\xi\cos\phi & 1 \end{pmatrix}$
$\alpha(b)$	$\begin{pmatrix} \beta & \eta\xi\sin\phi & 0 \\ -\eta\xi\sin\phi & \beta & 0 \\ \eta\xi\cos\phi & \eta\xi\cos\phi & 1 \end{pmatrix}$	$\begin{pmatrix} \beta & 0 & \eta\xi\cos\phi \\ \eta\xi\sin\phi & 1 & \eta\xi\sin\phi \\ -\eta\xi\cos\phi & 0 & \beta \end{pmatrix}$
$\beta(b)$	$\begin{pmatrix} \beta & \eta\xi\cos\phi & 0 \\ -\eta\xi\cos\phi & \beta & 0 \\ \eta\xi\sin\phi & \eta\xi\sin\phi & 1 \end{pmatrix}$	$\begin{pmatrix} \beta & 0 & \eta\xi\sin\phi \\ \eta\xi\cos\phi & 1 & \eta\xi\cos\phi \\ -\eta\xi\sin\phi & 0 & \beta \end{pmatrix}$

$\beta = (1-\gamma^2)/(1+\gamma^2)$; $\xi = q\gamma/(1+\gamma^2)$

$\gamma = |\mathbf{M}_\perp|/N$; $F_N(\mathbf{Q}) = N\cos\phi + \imath N\sin\phi$

q is $+1$ if $\mathbf{M}_\perp$ is parallel to $\mathbf{y}$ or $\mathbf{z}$, and -1 if it is antiparallel.

Magneto-electric crystals

The property of magneto-electricity in centrosymmetric crystals is restricted to those having antiferromagnetic structures with zero propagation vector in which the centre of symmetry is combined with time-reversal. These are just the requirements for J_{ni} in Eq.2.13 and Eq.2.14 to be finite giving rise to off-diagonal terms P_{xz}, P_{zx} in the polarisation matrix. The origin can be chosen to make F_N real, in which case $\mathbf{M}_\perp$ is pure imaginary, and $J_{ni} = 2F_N M_{\perp i}$.

Although the temperature dependencies of magneto-electric (ME) susceptibilities are unique to each material, their magnitudes and even their signs are specimen dependent. This specimen dependence is due to the existence of 180° domains which have opposite ME effects. The measured ME susceptibility χ_{obs} is related to the intrinsic susceptibility χ_0 by

$$\chi_{obs} = \eta\chi_0 \tag{4.7}$$

where η is the domain fraction defined in Eq.4.6. SNP makes it possible, for the first time, to obtain the intrinsic ME susceptibilities since it allows the domain fraction η to be determined.

For a centrosymmetric ME crystal with domain fraction η and moments in the $\mathbf{x}$-$\mathbf{y}$ plane the polarisation matrix can be simplified to

$$\mathbf{P} = \begin{pmatrix} \beta & 0 & \eta\xi \\ 0 & 1 & 0 \\ -\eta\xi & 0 & \beta \end{pmatrix} \quad \text{with} \quad \begin{aligned} \beta &= (1-\gamma^2)/(1+\gamma^2) \\ \xi &= 2q_z\gamma/(1+\gamma^2) \\ \gamma &= |\mathbf{M}_\perp(\mathbf{Q})|/F_N(\mathbf{Q}) \end{aligned} \tag{4.8}$$

q_z is $+1$ if $\mathbf{F}_\mathbf{M}(\mathbf{Q})$ is parallel to $\mathbf{z}$, and -1 if it is antiparallel.

- Measurement of the polarisation matrix allows both η and γ to be determined.
- The absolute directions of rotation of the neutron spins when $\eta \neq 0$ determine the magnetic configuration of the more populous domain which allows the effects of electric and magnetic fields on the domain population to be studied.
- The results can shed light on the fundamental mechanisms leading to the ME effect.

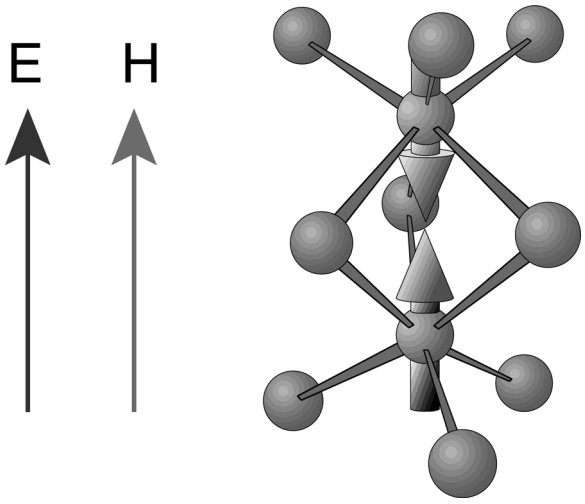

Figure 13. The pair of face sharing octahedra coordinating the Cr^{3+} ions in Cr_2O_3 showing the relative direction of spins stabilised by parallel electric and magnetic fields.

Cr_2O_3 is perhaps the best known ME material. The Cr^{3+} ions are octahedrally coordinated by oxygen and the structure is made up of pairs of octahedra, sharing a common face. These double octahedra are linked to others by sharing their free vertices. SNP has shown that electric and magnetic fields, applied parallel to one another and to the **c**-axis while cooling through the Néel transition, stabilise the domain in which the moments point towards the shared face of their coordinating oxygen octahedra as indicated in Figure 13.

5 SNP FOR DETERMINING PRECISE MAGNETIC STRUCTURE FACTORS

5.1 Magnetic structure factors from rotation of polarisation

The polarisation matrices given by Eq.4.8 for reflections from crystals in which the magnetic and nuclear scattering are in quadrature depend just on the ratio γ between the magnetic and nuclear structure factors and on the imbalance η in the populations of the two 180° domains. This property can be exploited in order to obtain precise values for the magnetic structure factors and hence for the antiferromagnetic form factor [10]. The polarisation matrix allows two independent estimates of γ to be obtained one from each of Eq.5.1(a) and Eq.5.1(b). (a) is only useful if there is an imbalance η in the population of 180° domains.

$$\text{(a)} \quad \mathsf{P}_{xz} = -\mathsf{P}_{zx} = \eta\xi = \frac{\eta q_y \gamma}{1+\gamma^2} \qquad \text{(b)} \quad \mathsf{P}_{xx} = \mathsf{P}_{zz} = \beta = \frac{1-\gamma^2}{1+\gamma^2} \tag{5.1}$$

5.2 Experimental considerations

The precision with which γ can be determined depends on the statistical error in the determination of $\mathbf{P}$. In this type of structure, the cross-section is independent of the polarisation direction. The counting rate

summed over the two polarisation states accepted by the detector is constant and independent of either the incident or the scattered polarisation direction. The polarisation measured by the analyser is given by:

$$P = (I^+ - I^-)/(I^+ + I^-) \tag{5.2}$$

where I^+ and I^- are the counting rates in the two detector channels.

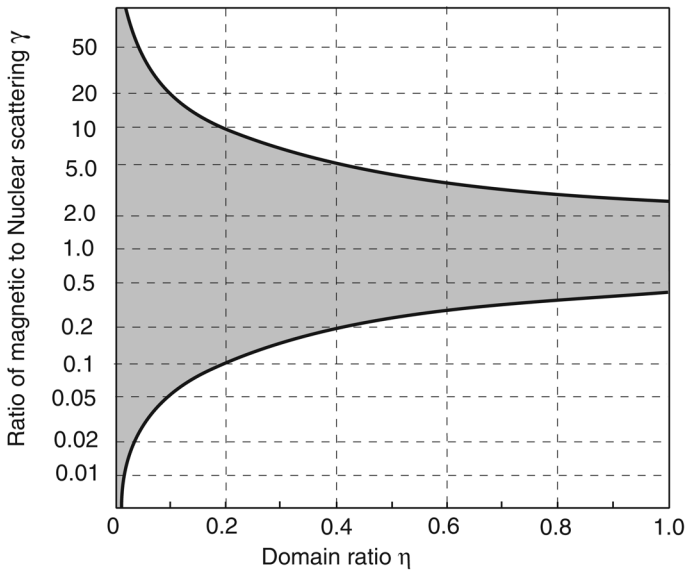

Figure 14. Plot of γ-η space. The shaded region is that in which Eq.5.1(a) gives a more precise estimation of γ than Eq.5.1(b). The γ axis is plotted on a logarithmic scale.

- The variance in the measurement of a component of polarisation due to counting statistics is

$$V_P = \frac{(1-P^2)^2}{4}\left(\frac{1}{N^+} + \frac{1}{N^-}\right) \tag{5.3}$$

  where N^+ and N^- are the counts recorded in each channel.
- The variance is minimised by dividing the measuring time available in the ratio $t^+/t^- = (1-P)/(1+P)$.
- With this division, if the total number of neutrons counted is N the variance becomes

$$V_P = (1-P^2)/N \tag{5.4}$$

- The variances in the values of γ derived from Eq.5.1(a) and Eq.5.1(b) are

$$\text{(a) } V_\gamma = \frac{(1+\gamma^2)^4}{16\gamma^2}V_P \quad \text{and} \quad \text{(b) } V_\gamma = \frac{(1+\gamma^2)^4}{4\eta^2(1-\gamma^2)^2}V_P \tag{5.5}$$

Figure 14 shows the areas in the γ-η plane where one or other of Eq.5.1(a) or 5.1(b), gives the more precise value for γ. If η is small (nearly equal domains) or γ is close to unity, the best estimate of γ will be obtained from Eq.5.1(b). For very small or very large γ Eq.5.1(a) will give a better value so long as η is not too small.

5.3 Determination of the Cr^{3+} form factor in Cr_2O_3

The polarisations scattered by a set of $h0l$ reflections from Cr_2O_3 have been measured with the crystal in several states with different domain populations produced by field cooling. Points on the Cr^{3+} form factor were obtained by multiplying the experimental γ values by the ratio between the nuclear structure factor and the geometric Cr site structure factor. The result is shown in Figure 15. For most reflections an extremely good precision was obtained. Exceptions are the $2, 0, \bar{2}$ and $1, 0, \bar{1}0$ reflections. For $2, 0, \bar{2}$ the nuclear structure factor is very small so that $\gamma >> 1$. For $1, 0, \bar{1}0$ the geometric structure factor for the Cr sites is small so the reflection is insensitive to the form factor. The data have also been used to make a maximum entropy reconstruction of the antiferromagnetic magnetisation distribution. Figure 16 shows the difference between the experimentally determined distribution and that calculated for an antiferromagnetic arrangement of Cr^{3+} ions with t_{2g} symmetry. It can be seen that there is a gradient of magnetisation at the Cr^{3+} positions. This may be the signature of the ME effect.

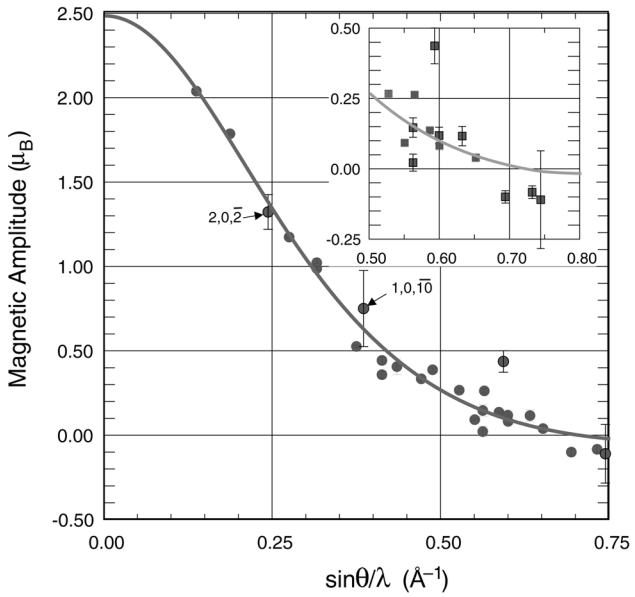

Figure 15. The experimental values of the magnetic form factor measured at the $h0l$ Bragg reflections of Cr_2O_3. The smooth curve is the spin-only free-ion form factor for Cr^{3+} normalised to the experimental value at the lowest angle reflection (10.2).

6 SUMMARY

- The scattered neutron polarisation is particularly sensitive to the directions of magnetic moments.
- For a pure system (no domains), SNP will determine the directions of the magnetic interaction vectors.
- SNP can distinguish true depolarisation, due to the presence of domains, from rotation of the polarisation by scattering.
- Any depolarisation which is found will characterise the types of domain which are present.
- Rotation of the polarisation towards, or away from, the scattering vector indicates some degree of chirality either in the magnetic structure itself or in its relationship with the nuclear structure.
- SNP cannot be used in isolation to determine magnetic structures with non-zero propagation vectors.

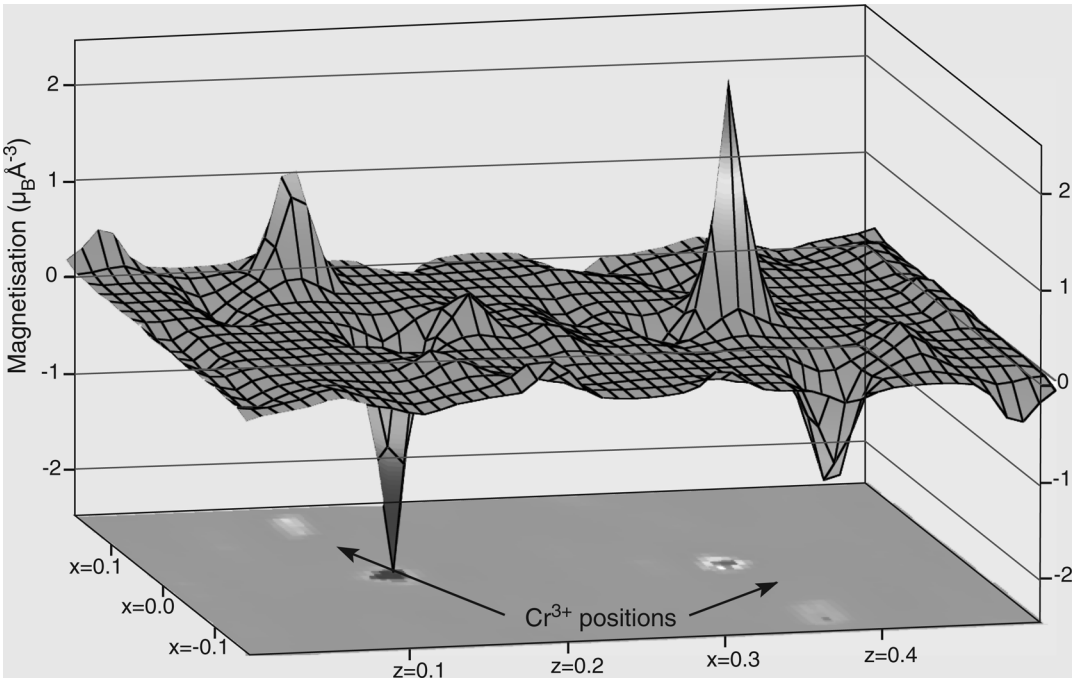

Figure 16. A maximum entropy reconstruction of the difference between the experimental magnetisation distribution in Cr_2O_3 and that calculated for an antiferromagnetic arrangement of Cr^{3+} ions with t_{2g} symmetry.

- Measurement of the polarisation matrices of a very few magnetic reflections are usually sufficient to determine the moment directions.
- When the phase relationship between the magnetic and nuclear structures can be controlled, SNP can be used to obtain precise magnetic structure factors.

References

[1] Blume, M., *Phys. Rev*. **130** 1670 (1963).
[2] Maleev, S.V., Bar'yaktar V.G. and Suris P.A., *Sov. Phys. - Solid State* **4** 2533 (1963).
[3] Forsyth, J.B., Brown, P.J. and Wanklyn, B.M., *J. Phys. C* **21** 2917 (1988).
[4] Brown, P.J., *et al., J. Phys. Condens. Matter* **3** 4281 (1991).
[5] Brown, P.J., Forsyth, J.B. and Tasset, F., *J.Phys. Condens. Matter* **10** 663 (1998).
[6] Robinson, R., *et al.*, *Phys. Rev. B* **47** 6138 (1993).
[7] Mannix, D., *et al.*, *Phys. Rev. B* **62** 3810 (2000).
[8] Yakel, H.L., Koehler, W.C., Bertaut, E.F. and Forrat, E.F., 16 **957** 1963 (Acta Cryst.).
[9] Bacon, G.E., *Neutron Diffraction* OUP Oxford (1975)pp 488–495.
[10] Brown, P.J., Forsyth, J.B. and Tasset, F., *Physica B* **267–268** 215 (1999).
[11] Brown, P.J., Forsyth, J.B., Lelièvre-Berna, E. and Tasset, F., *J.Phys. Condens. Matter* **14** 1957 (2002).